Effect of A-site ionic size variation on TCR and electrical transport properties of $(Nd_{0.7-x}La_x)_{0.7}Sr_{0.3}MnO_3$ with $x = 0, 0.1$ and 0.2

Effect of A-site ionic size variation on TCR and electrical transport properties of $(Nd_{0.7-X}La_X)_{0.7}Sr_{0.3}MnO_3$ with *x = 0, 0.1* and *0.2*

Sudarshan Vadnala[1], **Saket Asthana**[1,2], **Prem Pal**[1] **and S. Srinath**[3]
[1,2]Department of Physics, Indian Institute of Technology Hyderabad, India
[3]School of Physics, University of Hyderabad, India

E-mail: asthanas@iith.ac.in

Abstract. In this work, the structural and transport properties of $(Nd_{0.7-x}La_x)_{0.7}Sr_{0.3}MnO_3$ manganites with *x = 0, 0.1* and *0.2* prepared by solid state reaction route are studied. These compounds are found to be crystallized in orthorhombic structural form. Experimental results showing a shift in the metal to semiconductor/insulator transition temperature (T_{MI}) towards room temperature (289 K) with the substitution of Nd by La, as the value of *x* is varied in the sequence (*0,0.1,0.2*), have been provided. The shift in the T_{MI}, from 239 K (for *x=0*) to near the room temperature 289 K (for *x=0.2*), is attributed to the fact that the average radius $< r_A >$ of site-A increases with the percentage of La. The maximum temperature coefficients of resistance (TCR) of $(Nd_{0.7-X}La_X)_{0.7}Sr_{0.3}MnO_3$ (*x= 0.1* and *0.2*) are found to be higher compared to its parent compound $Nd_{0.7}Sr_{0.3}MnO_3$. The electrical transport mechanisms for $(Nd_{0.7-X}La_X)_{0.7}Sr_{0.3}MnO_3$ (*x= 0 to 0.2*) are explored by using different theoretical models, for temperatures below and above T_{MI}. An appropriate enlightenment for the observed behavior is discussed in detail.

1. Introduction

Pervoskite $AMnO_3$ type manganites have gained wide popularity because of their intriguing physical properties, resulting from the simultaneous presence of spin, lattice and orbital degrees of freedom [1-2]. These manganites have earned momentous attention from many researchers in order to seek their potential for spacious technological applications, e.g. read heads, magnetic information storage, low and high field magnetic sensors, infrared (IR) detectors and numerous other recent spintronic applications [3-10]. The fact that these substituted manganites procure high temperature coefficient of resistance (TCR) in bulk as well as in thin films at room temperature that makes them useful for infrared radiation detectors (i.e. IR detector) for night vision applications [11]. Among all perovskite manganites, $NdMnO_3$ is an antiferromagnetic insulator, characterized by a super exchange coupling between Mn^{3+} sites. This coupling is facilitated by a single e_g electron predominated by strong correlation effects. Partial substitution of Nd^{3+} ions with divalent cations (Sr, Ca and Ba) result in mixed valance states of Mn i.e. Mn^{3+}/Mn^{4+} which is responsible for the ferromagnetic Zener double exchange mechanism [12].

[2] Corresponding author: asthanas@iith.ac.in

The most prevalent experimental way of affecting the physical properties of manganites is by varying the ionic radii of A-sites. This creates structural distortions in manganites due to the size mismatch of A-site, which in turn generates the internal chemical pressure within the lattice. Due to this structural disorder effect, the local oxygen displacement occurs, ensuing into bond angle fluctuations and bond length variations, further leading to carrier localization in pervoskite lattice. This distortion can be controlled by the average size of the A-site cation which in turn modifies the Mn-O-Mn bond angle and Mn-O distances. The Mn-O-Mn bond angle is directly related to the hopping integral between Mn^{3+} and Mn^{4+} degenerate states. Thus, the variations in ionic radii at A-sites lead to competing phases at a particular temperature, hence influencing electrical and magnetic transport properties of the perovskite manganites.

In the present research, the structural and transport properties of Nd-based manganites with composition $(Nd_{0.7-x}La_x)_{0.7}Sr_{0.3}MnO_3$ (where $x = 0, 0.1$ and 0.2), are studied in order to tune the TCR and T_{MI} for IR detector applications.

2. Experimental details

The polycrystalline samples of $(Nd_{0.7-x}La_x)_{0.7}Sr_{0.3}MnO_3$, where x = *0*(NLSMO 0), *0.1*(NLSMO 1) and *0.2*(NLSMO 2) are synthesized by the solid state reaction route, using ingredients Nd_2O_3, La_2O_3, $SrCO_3$ and Mn_2O_3.The mixed powders are calcined, sintered and annealed(oxygen environment) at 1100 °C, 1300 °C and 1000 °C for 24hrs, 5hrs and 5hrs respectively. The structure and phase purity of the samples are analyzed by powder X-ray diffraction (XRD) and Raman spectroscopy. The resistivity measurement, without and with magnetic field of *5* tesla, are carried out using four-probe method in the temperature range from 5 to 300 K on a quantum design Physical Property Measurement System (PPMS).

3. Results & Discussion

3.1. XRD and Raman Spectra

XRD patterns of the polycrystalline manganites $(Nd_{0.7-x}La_x)_{0.7}Sr_{0.3}MnO_3$ ($x = 0, 0.1$and 0.2) exhibiting single–phase orthorhombic unit cell with *Pnma* (No *62*, PCPDF Ref No *861534*) space group are shown in figure1(a). It can be observed from the patterns that peaks are slightly shifted toward lower angle side on substitution of La in place of Nd. This small shift arises due to the mismatch of radius at A-site i.e., larger radius of La-ion (1.36 Å) in comparison to the radius of Nd-ion (1.27 Å) which causes increase in the volume of the lattice. Subsequently, an internal chemical pressure generated within the lattice due to size mismatch at A-site, which results in slight shift in the peaks of XRD pattern.

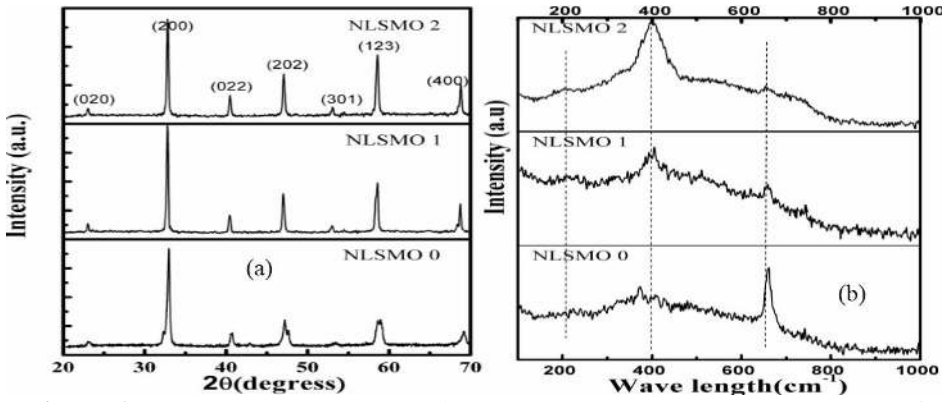

Figure 1. (a) XRD and (b) Unpolarized room-temperature Raman spectra of pervoskite manganites $(Nd_{0.7-x}La_x)_{0.7}Sr_{0.3}MnO_3$ where $x = 0, 0.1$ and 0.2.

The unpolarized room-temperature Raman spectra of $(Nd_{0.7-x}La_x)_{0.7}Sr_{0.3}MnO_3$ ($x = 0, 0.1$and 0.2) are shown in the figure1(b). Several phonon modes have been observed out of 24 allowed Raman

active modes in orthorhombic symmetry as per selection rule. The weak modes in the range 205-212 cm^{-1} presumably represent the rotational vibration of the MnO_6 [13]. The presence of two prominent peaks at 656 cm^{-1} and 406 cm^{-1} along with some weaker modes supports the orthorhombic symmetry as observed from XRD results. The modes in the range of 375-406 cm^{-1} occur due to the combined effects from the stretching vibration and Jahn-Teller (JT) distortion of the octahedra [14, 15]. A peak at 656 cm^{-1} is attributed to the bending vibration of octahedral which is also called as breathing mode. Broadening of this peak with La substitution confirms that robustness of JT distortion decreases with increasing $< r_A >$. Based on this argument, it can be attributed that all compounds crystallized with orthorhombic symmetry with slight variation in JT distortion with increasing La-content.

3.2. Electrical transport

The samples average radius of site-A increases from 1.321 Å (for $x = 0$) to 1.339 Å (for $x = 0.2$), T_{MI} shifts from 239 K (for $x = 0$) to 289 K (for $x = 0.2$) is shown in the figure 2a. It is worth to mention as average radius $< r_A >$ increases, the local lattice distortion reduces due to the shifting of Mn-O-Mn bond angle towards symmetrical side (approaches 180°). As a result, hopping amplitude increases which influence the T_{MI} shifts towards higher temperature.

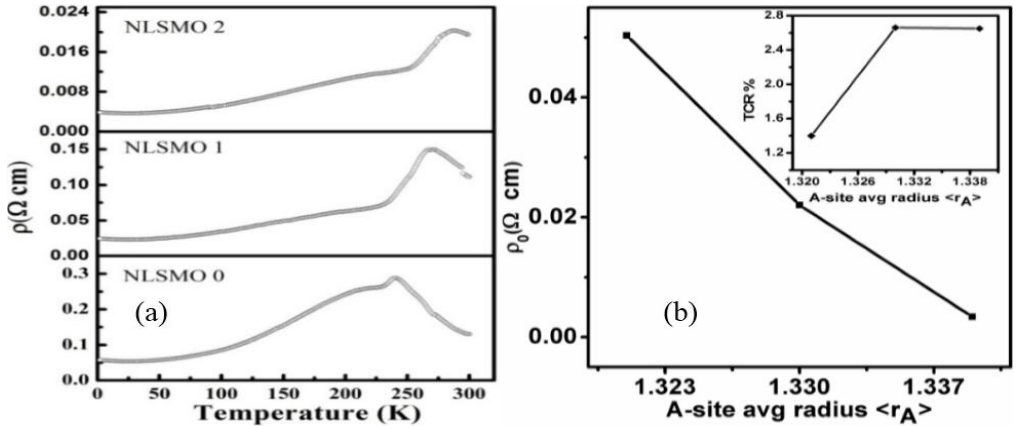

Figure 2. (a)Temperature dependent resistivity behavior of $(Nd_{0.7-x}La_x)_{0.7}Sr_{0.3}MnO_3$ where $x = 0, 0.1$ and 0.2 (b) residual resistivity vs A-site average radius.

The maximum %TCR $\left(TCR\% = \frac{1}{\rho}\left(\frac{d\rho}{dT}\right) * 100\right)$ vs average radius of A-site $< r_A >$ is given in the inset of figure 2(b). The maximum temperature coefficients of resistance (TCR) of $(Nd_{0.7-x}La_x)_{0.7}Sr_{0.3}MnO_3$ ($x = 0.1$ and 0.2) are found to be higher compared to its parent compound $Nd_{0.7}Sr_{0.3}MnO_3$. It is worth to mention here that %TCR has been optimized to a value of 2.66 (for $x = 0.1$) and 2.65(for $x = 0.2$) which are independent with $< r_A >$. This opens the possibility of further improvement in operating temperature for IR detectors applications without sacrificing an optimum %TCR value.

Below T_{MI}, temperature resistivity behavior is explained by using $\rho = \rho_0 + \rho_2 T^2 + \rho_{4.5} T^{4.5}$ general polynomial equation to fit the experimental data of our samples. In the equation, ρ_0 is the temperature independent residual resistivity which arises due to the grain/domain boundary effects, scattering by impurities, defects and domain walls [16, 17], $\rho_2 T^2$ describes the resistivity due to electron-electron scattering phenomenon [18]. The last terms $\rho_{4.5} T^{4.5}$ ascribes due to the process of electron-magnon scattering process in the ferromagnetic region. The residual resistivity ρ_0 is decreasing with increase of average radius of A-site is shown in figure 2(b).

On the other hand, in semiconducting regime ($T > T_{MI}$), the variation of resistivity with temperature is explained by an Adiabatic small polaron hopping $\rho = \rho_0 T \exp(\frac{E_P}{k_B T})$.The polaron hopping energy (E_P) decreases with increase of an average A-site ionic radius $< r_A >$ as shown in figure 3(a). A fitted curve on experimental data of NLSMO 0 by polaron hopping model is shown in an inset of the figure 3(a).

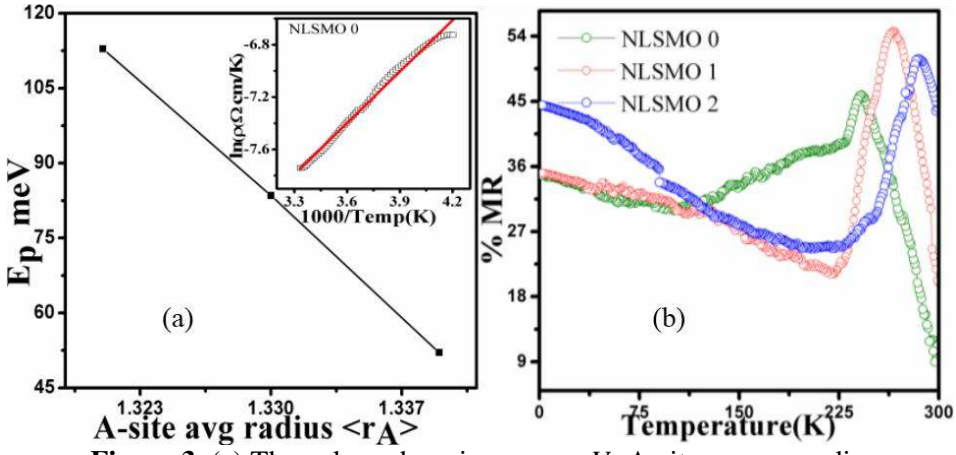

Figure 3. (a) The polaron hopping energy *Vs* A-site average radius
(b) Magnetoresistance *Vs* Temperature with in the field of 5 tesla.

The temperature dependent maximum percentage of magnetoresistance (%MR) at T_{MI} of compounds $(Nd_{0.7-x}La_x)_{0.7}Sr_{0.3}MnO_3$ are *46%* , *52%* and *50%* for $x = 0, 0.1$ and *0.2* with in the field of 5 Tesla. The low temperature MR is effect by the misalignment of adjacent magnetic domains/grains. Large magnetoresistance at T_{MI} is due to the misalignment of adjacent Mn ions and to the double exchange mechanism.

4. Conclusion

The metal-insulator transition (T_{MI}) temperature of $(Nd_{0.7-x}La_x)_{0.7}Sr_{0.3}MnO_3$ for $x = 0.2$ exhibits a shift towards room temperature as the average radius of site-A increases. Conduction mechanism is explained by the polynomial equation and by adiabatic polaron hopping model for low and high temperatures, respectively. Based on the results shown in this paper, it can be concluded that the residual resistivity (ρ_0) and polaron hopping energy decreases with an increase in the average radius of site-A. An interesting observation is that NLSMO 2 provides T_{MI} around the room temperature, and the maximum percentage change in TCR values are independent with average radius $< r_A >$ in $x = 0.1$ and $x = 0.2$.

References

[1] Coey J M D, Viret M and von Molnar S 1999 *Adv. Phys.* **48** 167
[2] Manh D H, Phong P T, Thanh T D, Hong L V and Phuc N X 2010 *J. Alloys Compd.* **491** 8
[3] Seikh Md M, Sudheendra L and Rao C N R 2004 *J. Solid State Chem.* **177** 3633
[4] von Helmolt R, Wocker J, Holzapfel B, Schultz M and Samver K 1993 *Phys. Rev. Lett.* **71** 2331
[5] Jin S, Tiefel T H, McCormack M, Fastnacht R A, Ramesh R, and Chen L H 1994 *Science* **264** 413
[6] Haghiri-Gosnet A M and Renard J P 2003 *J. Phys. D* **36** R127
[7] Heremans J 1993 *J. Phys. D: Appl. Phys.* **26** 1149
[8] Jin S, McCormack M, Tiefel T H and Ramesh R 1994 *J. Appl. Phys.* **76** 6929
[9] Mira J, Rivas J, Hueso L E, Rivadulla F, Lopez Quintela M A, Senaris M A Rodriguez and Ramos C A 2001 *Phys. Rev. B* **65** 024418

[10] Hueso L and Mathur N D 2004 *Nature* **427** 303
[11] Kim J H and Grishin A M 2005 *Appl. Phy. Letters* **87** 033502
[12] Zener C 1951 *Phys. Rev*. **82** 403
[13] Choi K-Y, Lemmens P, Guntherodt G, Pattabiraman M, Rangarajan G, Gnezdilov V P, Balahrishanan G, Mck Paul D and Less M R 2003 *J.Phys.:Condens. Matter* **15** 3333
[14] Kim K H, Gu J Y, Choi H S, Park G W and Noh T W 1996 *Phys. Rev. Lett.* **77** 1877
[15] Li Kebin, Li Xijun, Zhu Kaigui, Zhu Jingsheng and Zang Yuheng 1997 *J. Appl. Phys.* **81** 6943
[16] Snyder G J, Hiskes R, Dicarolis S, Beasley M R and Geballe 1996 *Phys. Rev. B* **53**, 14434
[17] De Teresa J M, Ibarra M R, Blasco J, Garcia J, Marquina C and Algarabel P A 1996 *Phys. Rev. B* **54** 1187
[18] Urushibara A, Moritomo Y, Arima T, Asamitsu A, Kido G and Tokura Y 1995 *Phys. Rev. B* **51**, 14103